# Modeling of Dynamic Phenomena in Small Hydropower Plant: Case Dobšina III - Slovakia

**Pavol Fedor, Daniela Perduková**

Faculty of Electrical Engineering and Informatics, Technical University of Kosice, 042 00 Kosice, Slovakia; pavol.fedor@tuke.sk, daniela.perdukova@tuke.sk

*Abstract: Small hydropower plants (SHPP) are increasingly recognized as key contributors to renewable energy production in the world, with low-impact on the environment. Their research and practical implementation are among the current tasks of modern energy engineering. The expected electricity production depends on specific design parameters of SHPPs, which can be evaluated by studying dynamic phenomena through specialized simulation models. The article explores the modeling of small hydropower plant systems employing an induction generator, with the objective of developing a tool for simulating their hydro-mechanical and electromagnetic phenomena, along with their mutual interactions. The proposed SHPP simulation model, incorporating a fuzzy-based efficiency model of its turbine, was validated using data from the real SHPP Dobšina III and subsequently applied to investigate the dynamics of fast electromagnetic phenomena during various operational modes of the SHPP as well as during short-term voltage outages in the electrical grid. Resolving this issue is essential for optimizing the design and operation of SHPPs and ensuring efficient electrical grid components, such as cables and circuit breakers. The obtained results validated the accuracy of the proposed SHPP model and demonstrated its universal applicability for addressing issues related to the optimal design of SHPP systems.*

*Keywords: small hydropower plant; fuzzy model of turbine efficiency, induction generator; experimental verification, electromagnetic phenomena*

# 1 Introduction

Small hydropower plants (SHPPs) are relatively simple and technically undemanding energy structures. Their significance in electricity generation has been steadily increasing worldwide over the past decades. Currently, they account for more than 2% of the total installed electricity capacity globally [1]. Typically producing up to 10 MW of electricity, small hydropower plants are emerging as a key renewable and sustainable energy source due to their flexibility and low environmental impact, supporting the integration of intermittent renewable sources such as wind and solar power. [2]. Compared to traditional energy sources such as coal, gas, and oil, the average costs associated with energy generation, operation,

and maintenance over their lifespan are significantly lower. SHPPs also have notable environmental and socio-economic impact, such as contributing to the mitigation of global warming, ozone depletion, and nuclear waste [3]. Consequently, research is increasingly focused on the design, control and optimization of SHPP electricity production in alignment with global trends and priorities in renewable energy utilization.

An important objective in the design of such energy systems is the optimization of electrical grid sizing during non-standard operating conditions, such as the start-up phases of SHPPs or short-term voltage drops in the electrical grid. Non-standard operation of SHPPs gives rise to undesirable phenomena, including an increase in generator current peaks, a drop in the angular frequency of the turbine shaft, and a reduction in the torque of the turbine shaft, among others, leading to operational failures and economic losses [4]. To address these challenges, it is essential to develop a functional simulation model of an SHPP, thoroughly investigate the dynamics of its fast electromagnetic phenomena, and analyze the interactions between the electrical grid and the hydraulic turbine. The results obtained can enhance the efficiency of control strategies and improve the design and sizing of individual components within SHPP systems.

Currently, various methods exist for modeling hydropower plants [5] [6] [7] [8]. Compared to these, the structure of SHPP models is simpler due to their smaller scale and more straightforward design. As a result, certain factors can be neglected, such as the effects of water wave time constants, the water hammer phenomenon, and the impact of surge chambers, among others [9] [10]. Differences among SHPP model types primarily arise from the complexity of modeling their individual components. This is particularly relevant for the modeling of hydraulic turbines and the type of model used for the electric generator.

When modeling hydraulic turbines, the key consideration is whether their relatively strong nonlinear characteristics are preserved or whether the authors of individual simulation schemes have opted for simplifications, such as linearizing the model around the operating point [11]. SHPP models that do not account for certain effects (nonlinearities) may be used to study the dynamic behavior of SHPPs influencing control design only for specific operational conditions or steady-state situations [12] [13]. The application of artificial intelligence methods in developing nonlinear models of the hydro-mechanical part of SHPPs presents a challenge for future research in this field.

The most commonly used type of electric generator in models of larger hydropower plants is the synchronous generator, due to its efficiency and the ability to control the power factor of the electrical grid through excitation [14]. The disadvantage of synchronous generators lies in their relatively complex control and synchronization with the electrical grid. In smaller systems, such as SHPPs, the efficiency of the electric generator is of lower priority, which is why induction generators are becoming more commonly used. These generators significantly reduce control

system costs and do not require additional excitation sources [15]. Induction generators are less efficient than synchronous generators in stable flow conditions, but they offer simpler construction and easier maintenance, what is more economically demanding [16].

The SHPP models presented in [7] [8] allow for the investigation of the properties of the dynamically slow hydro-mechanical part of the SHPP (whose time constants range from seconds to tens of seconds), which is crucial for the design of its control system. To analyze faster dynamic phenomena of the electric generator, the SHPP model must be supplemented with a detailed description of its electro-mechanical part, along with models of the mechanical coupling between the turbine and the generator and the electrical grid.

The article provides a brief description and models of the individual subsystems of an SHPP, from which its complete simulation model was constructed using MATLAB/Simulink. For the non-linear subsystem of the turbine, a model considering its efficiency based on fuzzy logic has been proposed. To model the dynamic phenomena of the electromechanical part of the SHPP, the IM model was used for the generator model instead of its simplified model based on the Kloss relation [5], [8], which is unsuitable for these purposes. The parameters of the simulation model correspond to real data from the SHPP Dobšina III, while the correctness of the design of its hydromechanical component was validated by experimental measurements.

The aim of the article is to analyze the dynamic properties of the electric generator of the small hydropower plant Dobšina III for basic operational modes of the SHPP. The current peaks that arise during transitions between these modes should not exceed values defined by the grid or its operator, as this influences the proper sizing of cables, circuit breakers, and other components of the electrical grid. The article demonstrates a method to limit these undesirable current peaks by appropriately inserting additional resistances into the stator of the electric generator for a short period.

# 2 Small Hydropower Plant Model

A small hydropower plant is a complex nonlinear dynamic system consisting of five main subsystems [8] (Fig.1). The basic subsystem of the entire SHPP is the hydraulic turbine, which converts water energy into mechanical energy. This conversion is controlled by the Governor subsystem, whose output signal represents the demand for water flow control in the Servodrive subsystem. The conversion of the turbine's mechanical energy into electrical energy is performed by a subsystem called the Electric generator, which can be a synchronous or induction electric machine. If a synchronous generator is used, its excitation must also be modeled by a separate subsystem.

The complete model of the SHPP is obtained by interconnecting the individual subsystems as shown in Fig. 1.

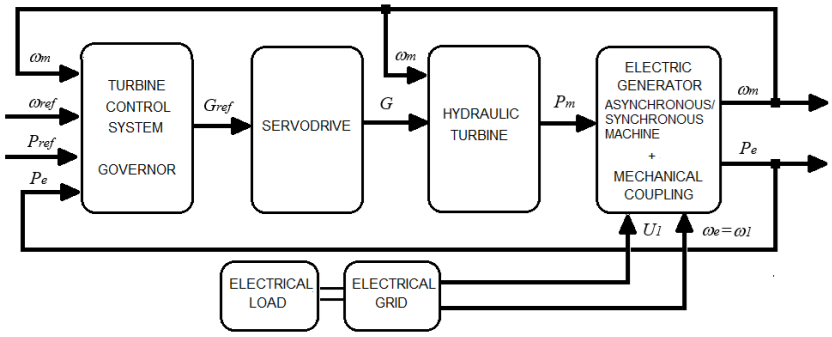


Figure 1
A small hydropower plant block diagram

Nomenclature:

$G$ guide vane opening position, [%]
$G_{ref}$ guide vane opening position reference value, [%]
$P_e$ electrical power of the generator, [W]
$P_{ref}$ turbine reference power, [W]
$P_m$ mechanical power on the turbine shaft, [W]
$\omega_e$ electrical grid angular frequency, [rads$^{-1}$]
$\omega_m$ mechanical angular speed of the shaft, [rads$^{-1}$]
$\omega_{ref}$ the reference value of the shaft angular speed which is the same as the electrical angular frequency of the grid, [rads$^{-1}$]
$\omega_1$ grid angular speed, [rads$^{-1}$]
$U_1$ grid voltage amplitude, [V]

The accuracy of the modeling of the individual subsystems depends on the purpose of use of the complete model. In the following chapters, the models of the individual subsystems of the SHPP are briefly described with respect to the structure and parameters of the specific SHPP Dobšina III. It consists of a Kaplan turbine with an output of 275 kW directly coupled to an induction generator with an output of 315 kW. The resulting model of this SHPP, the hydromechanical part of which was verified on the basis of experimental data, was used for modeling and analysis of its electromagnetic phenomena for various operating conditions. The input quantities and the waveforms of the output quantities are presented in the normalized form, which is characteristic of most of the published works [5] [8] [10].

## 2.1. Hydraulic Turbine Model

Due to its essential function in the overall power generation process, the hydraulic turbine (hereafter referred to as the turbine) is considered the heart of the

hydropower plant. The turbine model is a complex nonlinear dynamic system, some parameters of which are often obtained only by theoretical estimation.

The simulation scheme of the turbine model is shown in Fig. 2 [10], where $h$ is a water column head, $T_w$ is a water time constant, $q$ is the turbine water flow, and $P_{mideal}$ is the ideal mechanical power of the turbine without considering losses and efficiencies, which is not possible in real operating conditions.

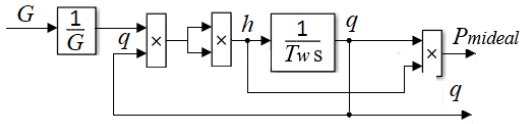


Figure 2
A hydraulic turnine simulation model

From the point of view of diagnostics and dynamic response of the whole hydropower plant to external influences, as well as from the point of view of correct way of its control, turbine models with consideration of its efficiency are important. These models differ in the approach of integrating the efficiency into the model and its effect on the mechanical power $P_m$ [17].

The authors in [10] [11] presented a model of a hydraulic turbine that accounts for its efficiency by its no-load flow rate. The quality of the model is affected by the exact knowledge of parameters such as the load damping constant or the hydraulic turbine gain, which are difficult to determine with the required accuracy.

Another approach published in [5] is based on the direct calculation of the turbine efficiency from the formula for calculating its mechanical power $P_m$

$$P_m = \eta \rho g q h = \eta \rho g P_{mideal} \tag{1}$$

where $\eta$ is the turbine efficiency, $\rho$ is the density of water and $g$ is the gravitational acceleration.

The turbine efficiency is calculated using the formula

$$\eta = \left[\frac{1}{2}\left(\frac{90}{\lambda_i} + q + 0.78\right) exp\left(\frac{-50}{\lambda_i}\right)\right](3.33q) \tag{2}$$

while $\lambda_i$

$$\lambda_i = \left[\frac{1}{(\lambda+0{,}089)} - 0.0035\right]^{-1} \tag{3}$$

and $\lambda$

$$\lambda = \frac{R_{blades} A_{blades} \omega_m}{q} \tag{4}$$

Equations (2)-(4) show that the efficiency is a non-linear function whose calculation depends on the exact values of important turbine design parameters such as the

radius of the turbine blades $R_{blades}$ and the size of the blade area $A_{blades}$. The exact values of these design parameters are often unknown and, in addition, they can change significantly during turbine operation [5].

If we know the values of the turbine efficiency $\eta$ in steady-state operation for each regularly distributed section of the defined working space of the quantities of mechanical angular speed $\omega_m$ and water flow $q$, then based on them we can compile the database shown in Table 2 It replaces the calculation of the turbine efficiency according to Eqs. (2)-(4). The values given in Table 1 are normalised to the experimentally measured values of $\omega_m$ and $q$ directly in the operation of the Dobšina III SHPP.

Table 1

Measured database at different steady state operation points

| **Efficiency** □ [p.u.] | | **Mechanical angular speed $\omega_m$** [p.u.] | | | | |
|---|---|---|---|---|---|---|
| | | **0.2** | **0.4** | **0.6** | **0.8** | **1** |
| **Waterflow $q$** [p.u.] | **0.2** | 0.13 | 0.30 | 0.36 | 0.38 | 0.38 |
| | **0.4** | 0.03 | 0.26 | 0.49 | 0.64 | 0.73 |
| | **0.6** | 0.04 | 0.14 | 0.41 | 0.67 | 0.87 |
| | **0.8** | 0.01 | 0.06 | 0.27 | 0.56 | 0.84 |
| | **1** | 0.00 | 0.02 | 0.16 | 0.42 | 0.72 |

Based on this database, which describes the relationships $[\omega_m, q] \rightarrow \eta$, a fuzzy model of turbine efficiency was designed using the anfisedit/MATLAB tool and the Subtractive Clustering method with default parameters (Range of influence = 0.5, Squash factor = 1.25, Accept ratio = 0.5, Reject ratio = 0.15). The result is a Sugeno-type static fuzzy system with 12 rules, the structure of which is shown in Fig. 3 and the characteristic surface in Fig. 4.

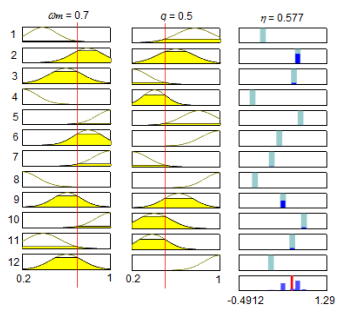


Figure 3

Sugeno type efficiency fuzzy model

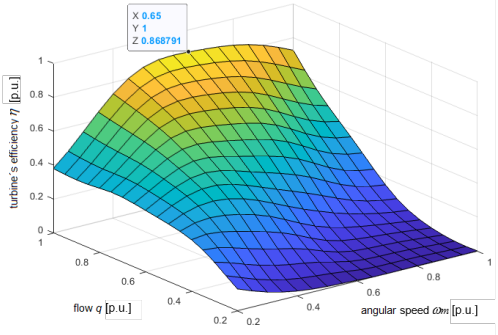


Figure 4

Characteristic surface of the fuzzy efficiency model

Using the default settings for the Subtractive Clustering method, the fuzzy systems showed a low approximation error (e ≈ 0.0015248). Adjusting other parameters of the Subtractive Clustering method was not necessary in this case, as the database used to create the fuzzy systems was of high quality (Table 1). The data was evenly distributed over the entire input workspace and exhibited monotonicity.

The resulting block diagram of the turbine model with the fuzzy efficiency model and the calculation of its mechanical power $P_m$ according to Eq. (1) is shown in Fig. 5.

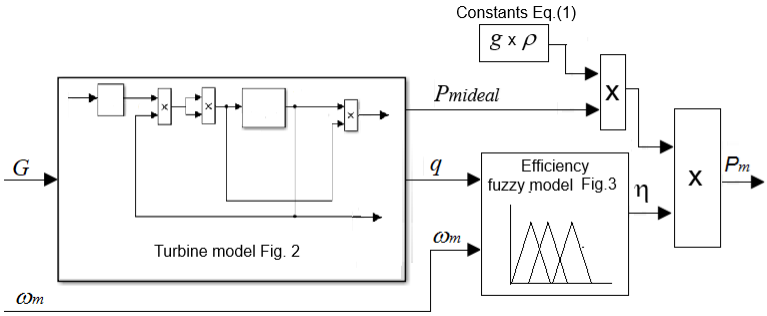


Figure 5
Turbine model with consideration of the fuzzy efficiency model

## 2.2 Servodrive Model

The Servodrive subsystem is the actuator for controlling the flow of water power to the turbine. According to the literature [10], its model is a 2nd order dynamic system (Fig. 6).

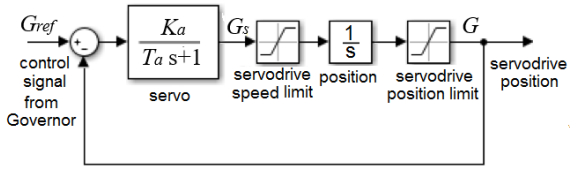


Figure 6
Servo drive subsystem block diagram

The input signal is the reference value of the actuator position $G_{ref}$, through which the controller compensates for the difference between the desired and actual turbine speed, or the output frequency of the system. The state variables are the speed of the guide vane opening $G_s$ and its position $G$ [%]. At higher levels of the water column above the turbine, strong pressure waves (water hammer) are generated when the guide vanes open and close, which can lead to damage to the turbine. Therefore, for safety reasons, the servodrive model limits the speed of their opening,

i.e. the speed of the water supply to the turbine. The limitation of the output position of the blades is used to set the realistic operating range in which the turbine still responds to the opening of the servo-drive. Both constraints are strongly nonlinear in nature. The constant $K_a$ is the gain of the servo-drive and $T_a$ is its time constant.

## 2.3 Turbine Control Model - Governor Subsystem

When developing our simulation model of a small hydropower plant, we used the knowledge gained from the description of various methods and procedures for the design of control structures for hydropower plants [5] [6] [7] and the available information on the control methods of the Dobšina III hydropower plant.

Turbine control basically has two basic functions:

1. Control of the turbine speed in the generator area.

2. Control of the power delivered to the grid (if required).

At the beginning of the control design, it is necessary to analyse the main dynamic events affecting the operation of the hydropower plant when the turbine is started up to the desired speed and connected to the grid, and to decide on the control design procedures based on their nature [6] [8].

The simplest model of turbine control (which also corresponds to SHPP Dobšina III) is the use of standard types of controllers in the circuit shown in Fig. 7 [8]. This structure contains two controllers - a speed controller $R_\omega$ of the PID type and a power controller $R_p$ of the PI type, whose output is the variable slip angle speed $\omega_2$.

The switching to power control is provided by the logic signal $d_{ref}$ (entered directly by the operator or from the control system). A first-order inertial filter with a time constant $T_f$ is included in the structure to avoid the undesired effects of rapid changes in the desired angular speed, thus optimising the control operation. When the turbine starts, the value of $\omega_{ref}$ may differ from $\omega_e$ because the electrical grid is not yet connected. When the angular speed of the turbine is synchronised with the electrical angular speed of the grid, the value of $\omega_{ref}$ is identical to $\omega_e$.

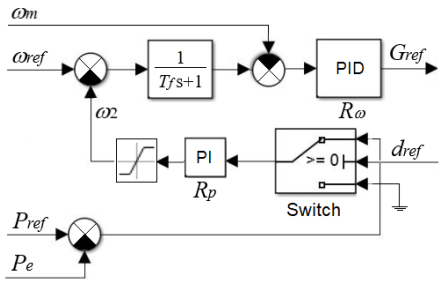


Figure 7
Block diagram of turbine control subsystem - Governor

## 2.4 Electromechanical Subsystem Model

An electric generator (hereinafter referred to as generator) is an alternating-current electric machine of the synchronous or induction type. The models of these machines are nonlinear dynamic systems of higher order, whose internal electromagnetic dynamic phenomena are in the range of milliseconds. On the other hand, the hydrodynamic phenomena in a turbine are much slower. For this reason, only the electromechanical model of the generator is often considered in terms of the moment equation on the common shaft of turbine and generator. The electrical part in this subsystem is the generator and the mechanical part is the shaft connecting the turbine and the generator. The block diagram of the electromechanical subsystem is shown in Fig. 8. The quantity $T_e$ represents the electrical torque of the generator.

The mechanical power of the hydraulic turbine is transmitted to the shaft (rotor) of the generator by a mechanical linkage. The stator of the generator is connected to a three-phase electrical grid with voltage $U_1$ and frequency $f_1$. When the turbine turns the shaft of the generator above the electrical angular speed of the grid $\omega_e$ (i.e., the slip of the induction motor is greater than 1), power from the turbine begins to be delivered to the grid. Since the turbine shaft always has a mechanical turbine speed, the mechanical power of the turbine $P_m$ minus the losses in the induction generator will be equal (in steady state) to the electrical power of the generator $P_e$ delivered to the grid.

### 2.4.1 Model of the Mechanical Coupling between Turbine and Generator

The model of the coupling of the generator-turbine subsystem (load) according to the literature [10] is shown in Fig. 9, where $T_m$ is the mechanical torque of the turbine proportional to its mechanical angular speed $\omega_m$; the constant $T_t$ represents the friction torque taking into account the friction losses, the quantity $J_c$ is the total torque of inertia of the system (turbine+shaft+generator), $T_r$ represents the time constant of the rotor of the induction generator corresponding to the resistance of its rotor.

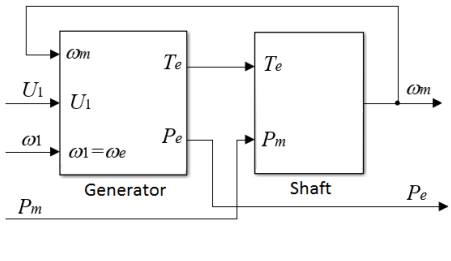


Figure 8
Block diagram of generator and turbine interconnected on a common shaft

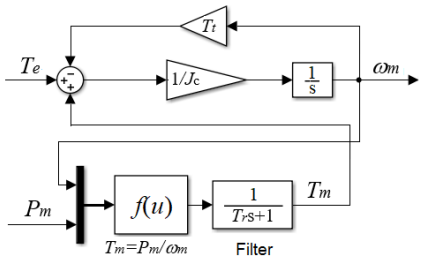


Figure 9
Block diagram of the generator-turbine model

### 2.4.2 Model of the Generator

In the SHPP model, an induction machine (IM) was used as the generator. In case we want to model the electromechanical phenomena of the SHPP, we can use a simplified induction generator model. Its electrical torque is modeled in a simplified way based on the Kloss relation: [18]

$$T_e = \frac{2U_1 s s_{max}}{s^2 + s_{max}^2} \tag{5}$$

A block diagram of such a model is shown in Fig. 10, where $s$ and $s_{max}$ are the slip and maximum slip of the IM and $n_p$ is the number of its poles. The IM electrical power at the shaft $P_e$ is proportional to the product of its torque $T_e$ and the mechanical angular speed of the shaft $\omega_m$.

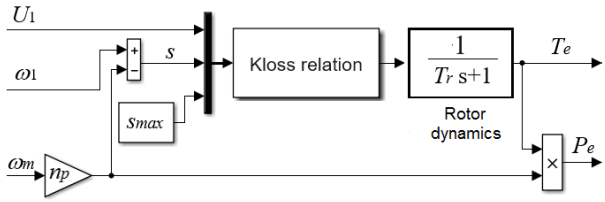


Figure 10
Block diagram of the simplified IM model as a SHPP generator

If the modelling objective is also to investigate fast electromagnetic phenomena in the generator, then it is appropriate to use a complete dynamic model of the induction machine.

Several dynamic IM models are known in the literature depending on the choice of state variables and rotating coordinate system [19] [20]. The state description of the current-flow model of a 3-phase short-circuit induction motor in a reference coordinate system {x,y}, is as follows [21]

$$\begin{bmatrix} \frac{di_{1x}}{dt} \\ \frac{di_{1y}}{dt} \\ \frac{d\psi_{2x}}{dt} \\ \frac{d\psi_{2y}}{dt} \end{bmatrix} = \begin{bmatrix} -\omega_0 & \omega_1 & -K_{12}\omega_g & -K_{12}\omega_m n_p \\ -\omega_1 & \omega_0 & K_{12}\omega_m n_p & -K_{12}\omega_g \\ M\omega_g & 0 & -\omega_g & \omega_2 \\ 0 & M\omega_g & -\omega_2 & \omega_g \end{bmatrix} \begin{bmatrix} i_{1x} \\ i_{1y} \\ \psi_{2x} \\ \psi_{2y} \end{bmatrix} + + \begin{bmatrix} K_{11} & 0 \\ 0 & K_{12} \\ 0 & 0 \\ 0 & 0 \end{bmatrix} \begin{bmatrix} u_{1x} \\ u_{1y} \end{bmatrix} \tag{6}$$

$$n_p \frac{T_m}{L_2} \left( \psi_{2x} i_{1y} - \psi_{2y} i_{1x} \right) - T_{load} = J \frac{d\omega_m}{dt} \tag{7}$$

The block diagram of IM model (Eq. 6, Eq. 7) is shown in Fig. 11.

Figure 12 shows a comparison of the electrical torque $T_e$ of the complete and simplified induction generator models at the basic operating modes of the SHPP:

Start-up, $t$=<0, 50> s; Grid connection, $t$=<50, 100> s; Power switching, $t$=<100, 200> s.

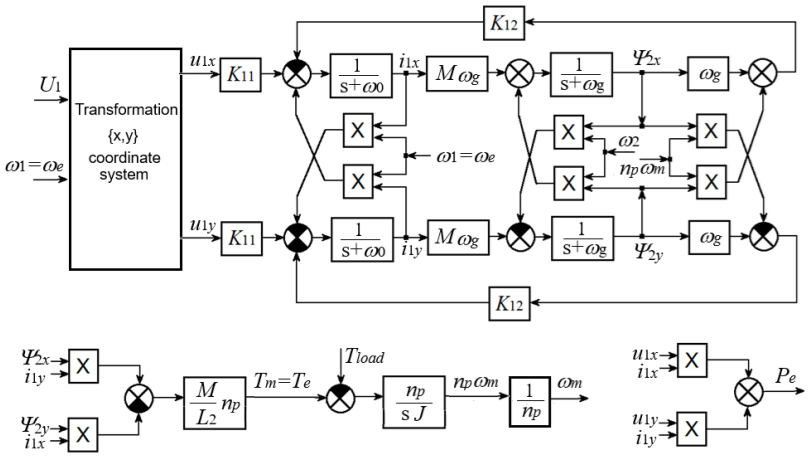


Figure 11

Block diagram of the complete dynamic IM model

Nomenclature:

$i_{1x}$, $i_{1y}$ - components of stator current vector $\boldsymbol{I}_1$, $u_{1x}$, $u_{1y}$ - components of stator voltage vector $\boldsymbol{U}_1$

$\psi_{2x}$, $\psi_{2y}$ - stator and rotor magnetic flux components, $\omega_m$ - motor mechanical angular speed

$\omega_1$ - angular frequency of the stator voltage, $\omega_1 = 2\pi f_1$ $\omega_2$ - slip angular speed, $\omega_2 = \omega_1 - \omega_m$

$R_1$, $R_2$ - stator/rotor phase resistance, $L_1$, $L_2$ - leakage inductances, $\omega_g$ - constant, $\omega_g = R_2/L_2$

$T_m$ - motor mechanical torque, $T_{load}$ - load torque, $n_p$ - number of pole pairs, $J$ - moment of inertia

$L_m$ - main inductance, $M$ - mutual inductance, $M = 2/3\, L_m$

$K_{11}$ constant, $K_{11} = 3/2\,[L_1 + L_2 L_m/(L_m + L_2)]^{-1}$

$K_{12}$ constant, $K_{12} = -3/2\,(L_1 + L_2 + L_1 L_2/L_m)^{-1}$

$\omega_0$ constant, $\omega_0 = K_{11}\,[R_1 + (M/L_2)^2\, R_2]$

In the start-up phase of the SHPP at the electrical angular speed of the grid $\omega_e$, the generator generates only the passive torque of inertia and the frictional torque on the turbine shaft, so its torque component $T_e$ delivered to the grid is zero.

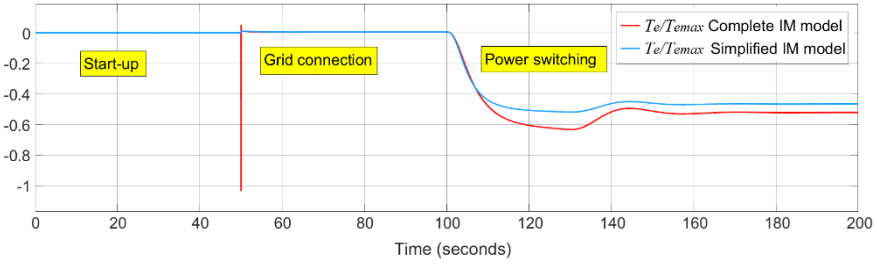


Figure 12

Comparison of torques and powers of the complete and simplified generator models

The biggest difference between these two models can be seen after the generator is connected to the grid (Grid connection) at time $t$=50 s. While the simplified IM

model shows practically no dynamic torque $T_e$ on the common shaft of the motor and turbine, the complete model shows short-term torque peak ($T_e$) which can reach up to the maximum allowed values in terms of torsional ratios on the turbine shaft and thus cause unwanted vibrations in its bearings. A detail of the generator connection to the grid is shown in Fig. 13.

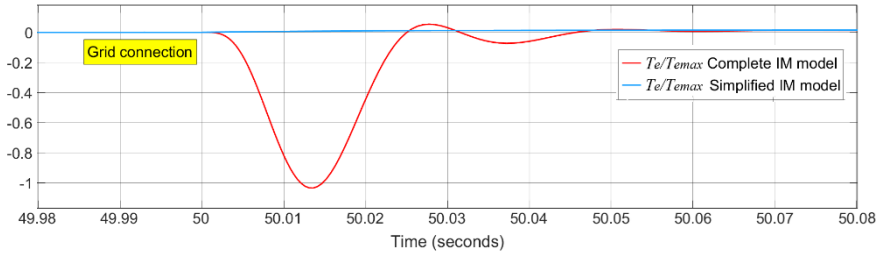


Figure 13
Detail of the generator connection to the electrical grid

# 3 Verification of the SHP Model Using Parameters from the Real SHPP Dobšina III

Based on the models of the basic subsystems of the SHPP presented in Chapter 2, a complete model of the SHPP according to Fig. 1 with an induction generator according to Fig. 11 was created. The hydromechanical part of this complete SHPP model was verified on real data from the SHPP Dobšina III. The parameters of the induction generator of the SHPP Dobšina III and the parameters of its hydromechanical subsystem are listed in the Appendix.

The accuracy of the simulation model was verified by comparing the mechanical angular speed of the turbine $\omega_m$, during its startup to the grid speed before the generator was connected to the electrical grid. Figure 14 shows the startup phenomena of the SHPP Dobšina III as recorded by the real operation control system. From the graph, it can be observed that the turbine accelerates to a speed corresponding to the grid frequency within $t = 25$ seconds, which is the duration of its transient state in real operation.

The mechanical angular speed $\omega_m$ of the turbine during its startup to the grid speed, obtained from the simulation model in MATLAB/Simulink, is shown in Fig. 15. Due to a different normalization of the variable $\omega_m$, its value of 60% corresponds to 100% in Fig. 14.

Note: The change in normalization for simulations was made to enable the simulation of certain fault operating conditions, during which the turbine's angular speed $\omega_m$ can significantly exceed the angular speed of the electrical grid $\omega_e$.

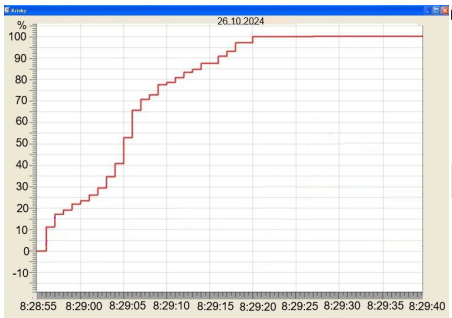


Figure 14
Startup of the SHPP Dobšina III from the control system

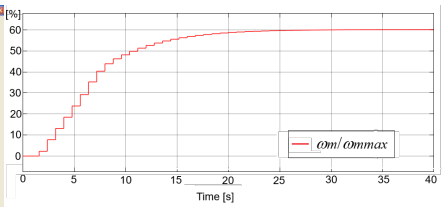


Figure 15
Startup of the SHPP Dobšina III from the simulation model

From Fig. 14 and Fig. 15, we can see that the time of the dynamic state of the turbine's mechanical angular speed $\omega_m$ during its startup to the grid speed are identical. This means that the turbine accelerates to the grid speed and is ready for the generator to be connected to the electrical grid within $t$ = 25 seconds. In this way, we validated the accuracy of the hydromechanical part of the simulation model, which includes all the properties of its subsystems, particularly the turbine model itself (including its nonlinearities) and the Governor subsystem (speed control).

The observed differences in the transient behavior of the mechanical angular speed $\omega_m$ could be caused by factors such as the output of the speed sensor installed in the SHPP Dobšina III. Additionally, the possible differences in the topology of its speed control system, details of which were not fully known to us.

The simulation model, validated with real data from SHPP Dobšina III, was subsequently used to simulate the dynamics of fast electromagnetic phenomena in the generator under selected operating conditions.

# 4 Modeling the Connection of a Generator to the Electrical Grid

Among the primary operational modes of SHPP is the connection (synchronization in the case of synchronous machines) of the generator to the electrical grid. To ensure this connection is as seamless as possible and does not induce undesirable dynamic effects (short-term electrical current peaks, peaks of torsional torque in the turbine shaft, increase of vibrations in the turbine bearings, etc.), the generator must be connected to the grid at the moment when the mechanical angular speed of the turbine $\omega_m$ is equal to the electrical angular speed of the grid $\omega_e$. This mode can

only be modeled in detail with a complete model of an induction generator (Fig. 11), as clearly demonstrated by the torque waveforms shown in Fig. 12 and Fig. 13.

Reducing current peaks in the generator can be achieved by temporarily inserting an additional stator resistance $R_1$ in series with the stator winding of the generator, which is a simpler and cheaper alternative than using inductors as a standard method. An example of modeling the impact of an additional stator resistance $R_1$=11 Ω for a duration of $t$=200 ms during the connection of the generator to the electrical grid at $t$=50 s, when $\omega_m=\omega_e$ is shown in Fig. 16. Such a procedure for controlling the grid connection mode makes it possible to reduce the transient current peaks and the peak torsional torque to approximately half the values in this particular case.

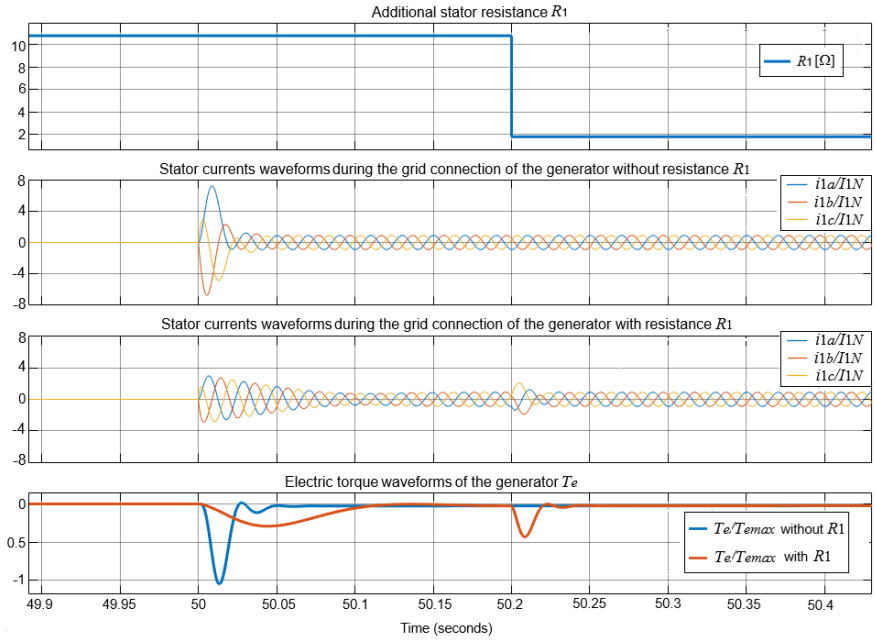


Figure 16

Detail of the generator connection to the grid with additional resistance $R_1$ if $\omega_m=\omega_e$

The quality of connecting the generator to the grid is also determined by the difference in angular speed between the turbine shaft $\omega_m$ and the electrical grid $\omega_e$. A simulation of connecting the generator to a slower electrical grid ($\omega_e$=95% $\omega_m$, $\omega_1=\omega_e$=0.57 rad/s at $t$=50 s is shown in Fig. 17. In such a case, inserting an additional stator resistance $R_1$ at the moment of grid connection significantly reduces current peaks. However, the peak torque on the shaft becomes much higher when this additional stator resistance is disconnected. In this case, it will be necessary to fine-tune its size and connection time.

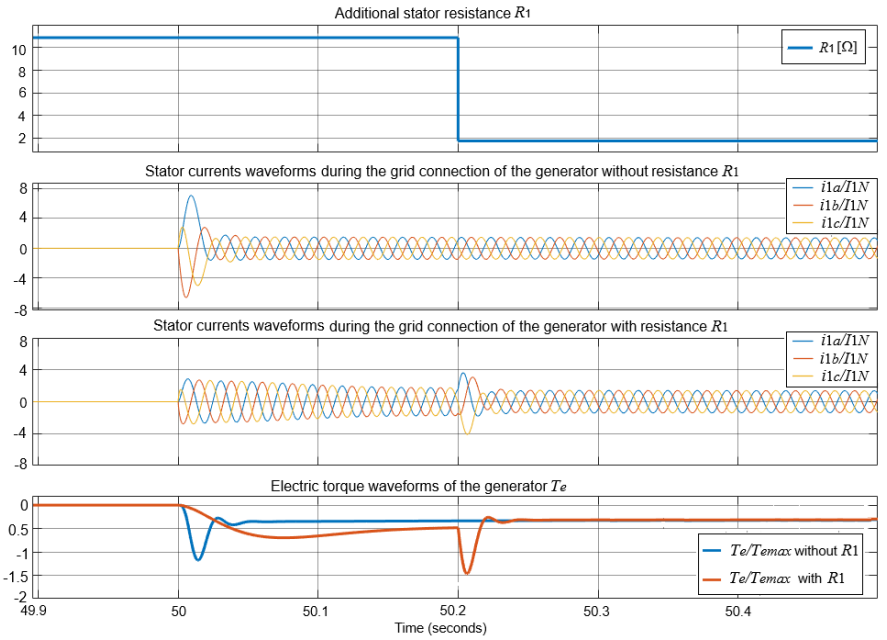


Figure 17

Detail of the generator connection to the grid with additional resistance $R_1$ if $\omega_e$=95% $\omega_m$,

# 5 Modeling of Short-Term Electrical Grid Outage

Another operational mode of the MVE is switching the turbine control from speed control to power control. This mode is simulated at time $t$=100 s from the turbine start-up. The stator current waveforms are influenced by the setting of the PI controller parameters for power control ($R_p$, Fig. 7) and do not exhibit significant peak values. Figure 18 shows the waveforms of selected SHPP variables for its primary operational modes. In this figure, it is evident that the output of the power controller (variable $\omega_2$-slip angular speed, Fig. 7) remains at its limit ($\omega_{2\text{lim}}$=0.1) for an extended period during the Power switching mode. Figure 18 also shows a simulation of a short-term electrical grid outage at time $t$=130 s during a period of $t$=0.5 s. It can be seen that this outage already has a significant impact on the fast electromagnetic phenomena in the generator (the peak values of its stator currents).

Since the power controller in the SHPP model is relatively slow and its output $\omega_2$ is limited, its setting does not have a significant impactt on the peak values of the generator currents. For example, if the proportional PI component of the power controller $R_p$ is changed twice ($K_p$=0.3), and its output limitation value is increased twice ($\omega_{2lim}$=0.2, Fig. 19 - variant 2) compared to the initial setting of its values

(Fig. 19 - variant 1). The detail of switching the control of the SHPP from speed control to power control at time $t$=100 s is shown in Fig. 19.

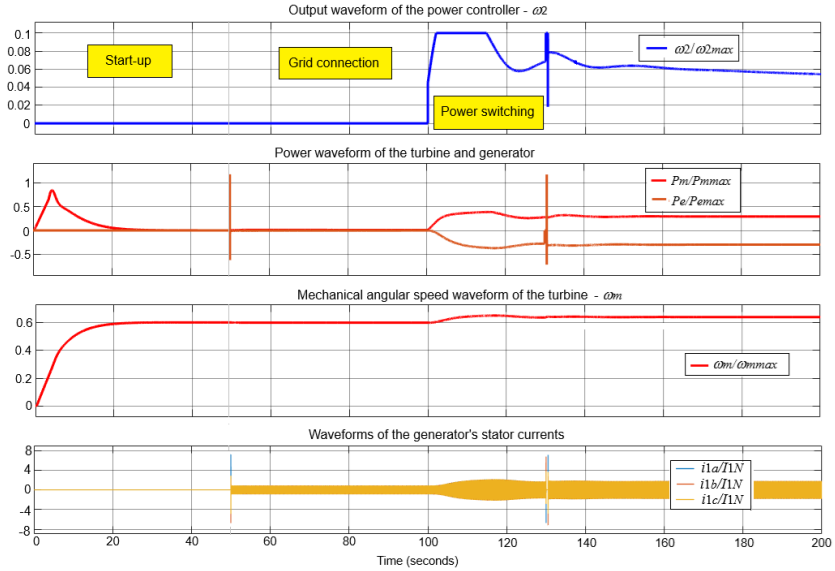


Figure 18

Waveforms of selected MVE variables during various operating modes

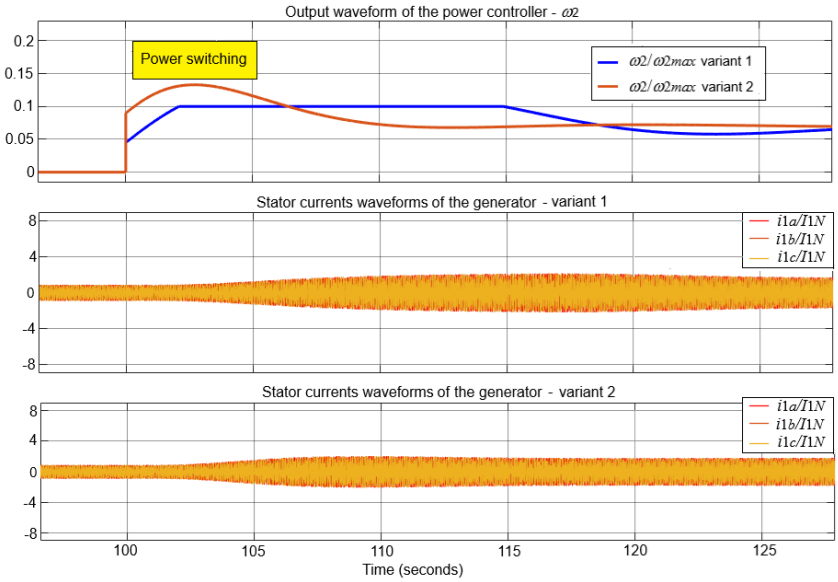


Figure 19

Effect of changing the power controller parameters on the current waveforms

The detail of the waveform of the generator stator currents during a short electrical grid outage in the operating mode Power switching for changes of the power controller parameters (variant 1, variant 2) is shown in Fig. 20. From this figure, it is evident that limiting the current peaks using additional resistances in the generator's stator is not possible at the moment of an electrical grid outage. The reason is that this transient process lasts on the order of tens of milliseconds, and the time for the closure of the power contactor, through which the additional stator resistances are connected, is also around 100 milliseconds. This means that the additional resistances would be connected to the generator's stator only at the time when its stator currents are already close to zero. However, with the additional stator resistances, we can limit these currents when the electrical grid is restarted.

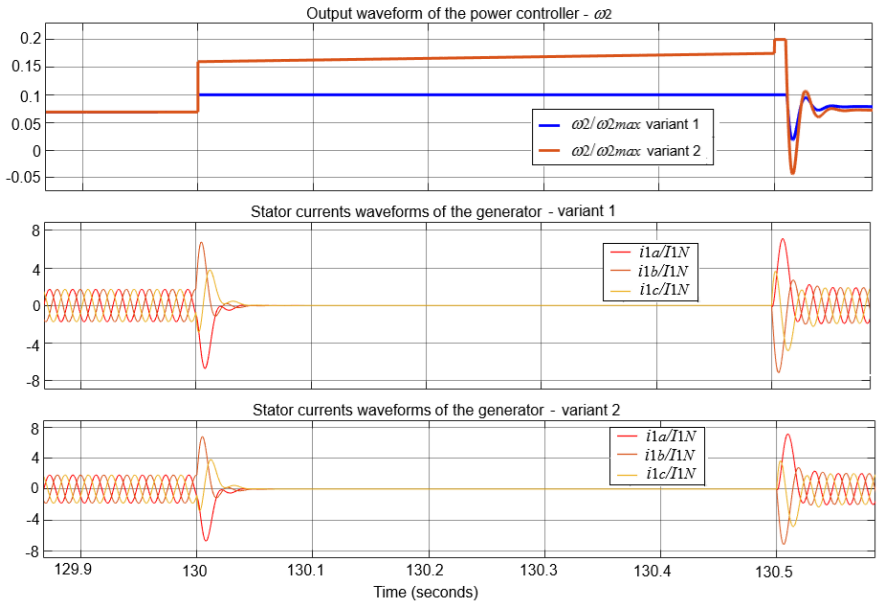


Figure 20

Detail of generator's stator current waveforms during a short-term power outage

Figure 21 shows a simulated condition when, after a short-term electrical grid outage at time $t = 130$ s, an additional resistance $R_1$ was connected to the generator's stator via a power contactor. The power contactor's closing time is $t = 100$ ms, so the inclusion of the additional resistance $R_1$ did not affect the peak currents of the generator during the electrical grid outage.

From Fig. 21 we can see that after the electrical grid restart at time $t = 130.5$ s, the additional stator resistance $R_1$ limits the current peaks during the generator's restart. However, when it is disconnected, the current peaks occur again, practically within the original range. The reason is the difference in the instantaneous mechanical angular speed of the turbine $\omega_m$ and the electrical angular speed of the grid $\omega_e$.

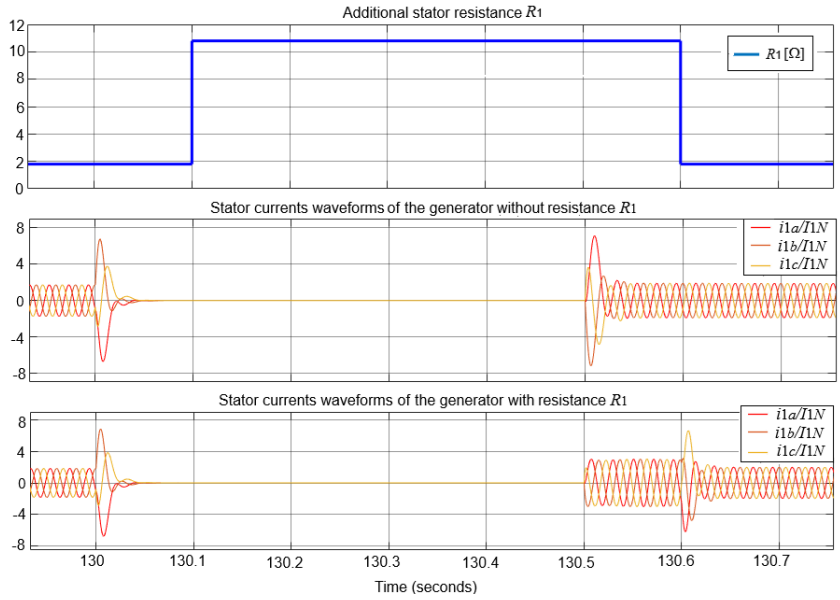


Figure 21
Detail of the generator's stator current waveforms during a short-term electrical grid outage

## Conclusion

The research presented successfully develops and validates a comprehensive simulation model for the small hydropower plant (SHPP) Dobšina III, emphasizing its hydromechanical and electromagnetic phenomena. The study integrates a fuzzy-based efficiency model for the hydraulic turbine and explores the dynamics of key operational modes, including generator grid connection and short-term voltage outages. The findings demonstrate the model's accuracy and applicability for optimizing SHPP design and operation, especially in mitigating undesirable transient effects such as current and torque peaks. The inclusion of additional stator resistance during specific phases proved effective in reducing these peaks, highlighting the potential for refined control strategies and sizing of individual components within SHPP systems such as cables and circuit breakers. This work highlights the significance of precise modeling in improving the efficiency and reliability of renewable energy systems, providing the way for advancements in SHPP technology and sustainable energy production.

## Appendix

Parameters of the induction generator:
$P_N$=315 kW, $J$=7.3 kgm$^2$, $\omega_g$=5.6106 s$^{-1}$, $U_{1N}$=400 V, $R_1$=0.01796 Ω, $\omega_0$=364.23 s$^{-1}$, $I_{1N}$=510 A, $R_2$=0.03656 Ω, $K_{11}$=1711.4 H$^{-1}$, $T_{mN}$=3126 Nm, $L_m$,0.00933 H, $K_{12}$=1632.9 H$^{-1}$, $n_N$=1011 revmin$^{-1}$, $M$=0.00622 H, $L_1$=$L_2$=0.00045 H, $n_p$=6
Parameters of hydromechanical subsystem

Hydraulic Turbine: $P_m$=275 kW, $T_w$=1.00594 s, $D$=0.0001 m, $A_t$=1.1992
Servo Drive: $K_a$=3.33, $T_a$=0.07 s, speed limit: <– 0.2; 0.2>, position limit: <0.01; 0.975>
Governor: $T_f$=4 s, Speed controller $R_\omega$ (PID): $K_P$=6.5, $K_I$=0.068, $K_D$=0;
Power controller $R_P$ (PI): $K_P$=0.15, $K_I$=0.1, $\omega_{2\text{lim}}$: <0; 0.1>;
Mechanical link: $J_c$=40 kgm$^2$, $T_r$=0.02 s, $T_t$=0.005 Nm

**Acknowledgement**

This work was supported by the Slovak Research and Development Agency under the Contract no. APVV-19-0210 and project VEGA 1/0363/23.

**References**

[1] N. Koltsaklis and J. Knapek, The Role of Flexibility Resources in the Energy Transition, *Acta Polytechnica Hungarica*, Vol. 20, No. 11, pp. 137-158, 2023, doi: 10.12700/APH.20.11.2023.11.9

[2] N. Bozsik, R. Magda, N. Bozsik, Analysis of Primary Energy Consumption, for the European Union Member States, *Acta Polytechnica Hungarica*, Vol. 20, No. 10, pp. 89-108, 2023, doi: 10.12700/APH.20.10.2023.10.6

[3] M. Kumar, *Social, Economic, and Environmental Impacts of Renewable Energy Resources, Wind Solar Hybrid Renewable Energy System*. IntechOpen, Feb. 26, 2020, doi: 10.5772/intechopen.89494

[4] A. Chauhan, R. P. Saini, A review on Integrated Renewable Energy System based power generation for stand-alone applications: Configurations, storage options, sizing methodologies and control, *Renewable and Sustainable Energy Reviews*, Vol. 38, 2014, pp. 99-120, doi: 10.1016/j.rser.2014.05.079

[5] A. Acakpovi, E. B. Hagan, and F. X. Fifatin, Review of Hydropower Plant Models, *International Journal of Computer Applications*, Vol. 108, No. 18, 2014, pp. 33-38, doi.10.5120/19014-0541

[6] N. Kishor and J. Fraile-Ardanuy, *Modeling and Dynamic Behaviour of Hydropower Plants*, London: The Institution of Engineering and Technology, 2017, p. 279, ISBN: 978-1-78561-195-7

[7] H. J. Wagner and J. Mathur, *Introduction to Hydro Energy Systems: Basics, Technology and Operation*. Heidelberg: Springer, 2011, ISBN 978-3-642-20708-2

[8] G. Munoz-Hernandez, S. Mansoor, D. Jones, *Modelling and Controlling Hydropower Plants*. London: Springer, 2013, ISBN 978-1-4471-6221-6

[9] D. Tsuanyo, B. Amougou, A. Aziz, B. N. Nnomo, D. Fioriti and J. Kenfach, Design models for small run-of-river hydropower plants: a review, *Sustainable Energy*, Vol. 10, No. 3, 2023, doi.10.1186/s40807-023-00072-1

[10] M. Sattouf, Simulation Model of Hydro Power Plant Using Matlab/Simulink, *International Journal of Engineering Research and Applications*, Vol. 4, No. 1, 2014, pp. 295-301, ISSN 2248-9622

[11] B. Xu, J. Zhang, M. Egusquiza, D. Chen, F. Li, P. Behrens, E. Egusquiza, A review of dynamic models and stability analysis for a hydro-turbine governing system, *Renewable and Sustainable Energy Reviews*, Vol. 144, 2021, 110880, doi: 10.1016/j.rser.2021.110880

[12] H. Goyal, T. S. Bhatti, D. P. Kothari, Control systems for small hydro-power plants: a review, *Int J Energy Technol Policy*, Vol. 5, No. 1, pp. 97-105, 2007, doi: 10.1504/IJETP.2007.012574

[13] D. Perdukova, M. Fedor, P. Fedor, Various Approaches for a Design of the Hydraulic Turbine Model, in: *11th International Scientific Symposium on Electrical Power Engineering, Elektroenergetika 2022*, 12.-14.9.2022, Stara Lesna, Slovakia, pp. 132-136, ISBN 978-805534104-0

[14] IEEE Guide for Synchronous Generator Modeling Practices and Parameter Verification with Applications in Power System Stability Analyses, in: *IEEE Std 1110-2019 (Revision of IEEE Std 1110-2002)*, pp. 1-92, 2 March 2020, doi: 10.1109/IEEESTD.2020.9020274

[15] K. Subramanya, R.Ch. Thanga, Capability of synchronous and asynchronous hydropower generating systems: A comprehensive study, *Renewable and Sustainable Energy Reviews*, Vol. 188, 2023, 113863, doi: 10.1016/j.rser.2023.113863

[16] C. P. Ion, C. Marinescu, Three-phase induction generators for single-phase power generation: An overview, *Renewable and Sustainable Energy Reviews*, Vol. 22, 2013, pp. 73-80, https://doi.org/10.1016/j.rser.2013.01.031

[17] Y. Zeng, L. Zhang, T. Xu and H. Dong, Building and Analysis of Hydro Turbine Dynamic Model with Elastic Water Column, in: *2010 Asia-Pacific Power and Energy Engineering Conference*, Chengdu, China, 2010, pp. 1-5, doi: 10.1109/APPEEC.2010.5449286

[18] J. Tiwari, A. Yadav, R. K. Jha and A. K. Singh, Modelling and Simulation of Hydro Power Plant using MATLAB & WatPro 3.0, *Intelligent Systems and Applications*, Vol. 7, No. 8, 2015, pp. 1-8, doi.10.5815/ijisa.2015.08.01

[19] G. Satyanarayana, M. Karthikeyan, R. Mahalakshmi and T. Vandarkuzhali, Vector Control of an Induction Motor for Speed Regulation, in *7th International Conference on Computing Methodologies and Communication* (ICCMC), Erode, India, 2023, pp. 1621-1625, doi: 10.1109/ICCMC56507.2023. 10084 248

[20] C. D. Tran, M. Kuchař, M. Sobek, V. Sotola and B. H. Dinh, Sensor Fault Diagnosis Method Based on Rotor Slip Applied to Induction Motor Drive, *Sensors*, Vol. 22, No. 22, 2022, art. no. 8636, doi.10.3390/s22228636

[21] D. Perdukova, P. Palacky, P. Fedor, P. Bober and V. Fedak, Dynamic Identification of Rotor Magnetic Flux, Torque and Rotor Resistance of Induction Motor, *IEEE Access*, Vol. 8, 2020, pp. 142003-142015, doi.10.1109/ACCESS.2020.3013944